

Effect of Grain Size on the Martensitic Transformation in CeO₂-Tetragonal Zirconia Polycrystals

by

Motozo HAYAKAWA, Hiroshi SHINMEN*¹, Muneo OKA,
Heizaburo NAKAGAWA*², and Ryoji INOUE*³

Department of Mechanical Engineering

- * 1 Graduate Student, Faculty of Engineering, Tottori University, Present Address : Japan Gore-tex Inc., Okayama Plant, Wake-gun, Okayama 709-02
- * 2 Department of Technology, Faculty of Education, Tottori University
- * 3 Hitachi Metals Co. Ltd., Yasugi Works, Yasugi-shi, Shimane 692

(Received September 1, 1991)

Effect of grain size on the tetragonal to monoclinic martensitic transformation was examined using 12mol%CeO₂-TZP (tetragonal zirconia polycrystals). The stability of the parent phase, as measured by martensite start temperature on cooling (M_s) or under applied stress (M_s^{σ}), decreased significantly with increasing grain size. Additional and the most significant change with increasing grain size was a decrease in the hardness. It was suggested that the average strength of the matrix would be the most critical factor controlling the nucleation of the martensitic transformation in the present system. Other possibilities which may influence the transformation were also discussed.

Key words : CeO₂-TZP, Martensitic Transformation, Nucleation, Grain Size Dependence, Zirconia

1. Introduction

Grain size dependence of the martensitic transformation is generally recognized both in metals and ceramics. In particular for transformation toughened ceramics, this dependence is a basis of retaining the high temperature tetragonal(t) phase in a critically metastable state at room temperature so that martensitic transformation to the stable monoclinic(m) phase would occur only in the high stress field around the tip of propagating cracks, thereby absorption of mechanical energy or equivalently toughening is achieved. Because of this technological importance and also because the phenomenon is closely related to the nucleation mechanism of martensite, the grain size dependence has received much study in the past. Although, the size dependence is observed both in powders (non-constraint particles) and bulk materials (constraint particles or grains), principal factors influencing the size dependence can be quite different. In powders, such factors as surface energy, surface contamination or adsorption, and the number and distribution of potential embryos may be important, whereas in bulk materials mechanical interaction between a transforming particle and its surrounding would play a dominant role. For this reason, these two cases need be treated separately, and in this article only the case of bulk materials shall be addressed. The transformation toughened ceramics are further classified into three groups, namely PSZ(partially stabilized zirconia),¹ TZP(tetragonal zirconia polycrystals),² and ZTA(zirconia toughened alumina).³ In the first two, particles of a metastable t-phase are embedded in the stable c-phase or alumina matrix, whereas in the last the material comprises only metastable t-phase of fine grains. The grain size dependence is generally recognized in all three groups and various models have been put forward to account for the mechanism of the grain size dependence.

One way of treating a transformation problem is to apply "end point" thermodynamics,⁴⁻⁶ where the transformation is assumed to take place when the free energy of the final state becomes lower than the initial state. If chemical free energy is the only energy term to be considered, the transformation is assumed to begin at T_0 , where T_0 is the temperature at which the initial and the final phases have the same chemical free energy. However, a variety of energy terms appear both in the initial and the final states. In the case of t-phase particles embedded in the stable cubic(c) phase or other stable matrix, the interfacial energy must be included in the free energy of the initial state. Additional energy may also appear from the strain misfit arising from different thermal expansion between the particle and the matrix. A free energy expression for the final state is generally more complicated depending on the degree of complexity of the assumed microstructure. The following effects have been considered by various authors in addition to elastic strain energy,

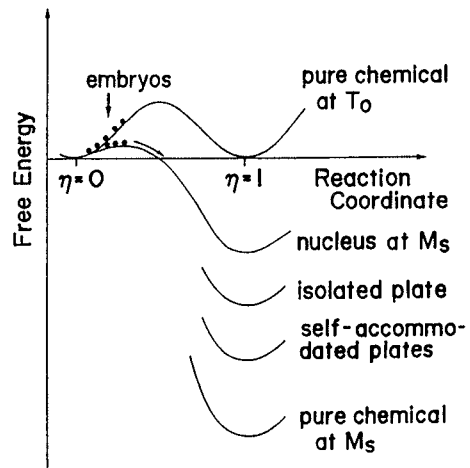


Fig. 1 Schematic diagram showing that the energy of martensite is dependent on the elastic state of final the structure but unrelated to the critical state of the nucleation. $\eta = 0$ and $\eta = 1$ represent the t- and m-lattice, respectively.

namely, particle/matrix interface energy,^{5,6} partial release of strain energy by the formation of twins⁴⁻⁶ and microcracks.⁵ In these treatments, the relative contributions of the above energy terms were considered to vary with particle size and thus result in the size dependence. These end point thermodynamic approaches were reported to account for the observed size dependence in some systems.⁴⁻⁶ However, it is not clear why this should be so, since in the usual reaction theory there exists an energy barrier between the initial and the final states as illustrated in a schematic diagram in Fig. 1. This barrier cannot be surmounted by a thermal activation process in the case of athermal martensitic transformation. Thus even if the free energy of the final state becomes lower than that of the initial state, transformation would not immediately take place. Instead, a further reduction in temperature is required so that the energy barrier is diminished until the most potent embryo starts to nucleate by falling down the potential downhill. The temperature giving this critical state defines M_s , the martensite start temperature. The energy of the nucleus must be considerably higher than the chemical free energy of the product phase owing to the dominant strain and interfacial energy. Once a nucleus is formed, its growth is rapid and spontaneous. Furthermore, such reaction often triggers activation of many other nuclei (a phenomenon known as autocatalysis) resulting in a burst transformation. All of this happens in a fraction of a second, often accompanying shattering of the specimen and evolution of significant heat. Still further, a reverse transformation temperature, A_s , is typically a few hundred degree higher than the forward transformation temperature, M_s . These facts clearly indicate that the free energy of the final state is significantly reduced from that of the initial nucleus. In addition, the amount of the energy reduction is largely dependent on the degree of strain accommodation as illustrated in Fig. 1. For these reasons, a direct comparison between the free energies of the initial and the final states is unlikely to provide any realistic criterion for the transformation.

Alternative way of approaching the problem is to consider factors influencing the nucleation. Anderson and Gupta⁷ assumed a statistically uniform distribution of embryos of varying potency. When a particle contains a potent embryo(s) at a fixed temperature, then the particle is considered to fully transform to the m-phase upon cooling to the temperature, but other particles free from a potent embryo remain untransformed. The probability that a particle contains at least one such potent embryo is proportional to the particle's volume since a uniform distribution is assumed. Thus, the larger is the particle size, the more easily the transformation would occur, which is an observed tendency of size dependence.

It is however difficult to clarify the nature of embryos and to quantify their potency and distribution. Furthermore a uniform distribution of embryos appear unlikely since nucleation is generally observed to take place at a particle interface or grain boundary. Still further, in the case of TZP, once nucleation takes place within a grain, the transformation would not be confined to the grain, instead extensive propagation into many other grains occurs by a burst. Thus if embryos are closely associated with grain boundaries, quite opposite tendency should be observed. For this reason, embryo theory alone cannot explain the observed tendency of the grain size dependence.

Heuer *et al.*⁸ studied the particle size dependence of transformation under transmission electron microscope using zirconia particles dispersed both inter- and intra-granularly in alumina matrix. They noted higher stability for the intra-granular particles than for the inter-granular particles of the same size. Since a higher stress was expected in the inter-granular particles than intra-granular particles by thermal expansion anisotropy, the authors pointed out the importance of residual stress. These authors also observed stabilization effect upon annealing and interpreted the result by annealing out of the defects on which nucleation would have taken place. They also observed the usual size dependence in the t-phase precip-

itates in Mg-PSZ. These authors suspected that the loss of coherency in the particle interface triggered nucleation, as suggested earlier by Hannink.⁹ It should be noted, however, that such coherent/incoherent transition is not expected in TZP, since the grain boundaries are inevitably incoherent.

Still another factor, which has not been considered for ceramics, is a strengthening effect arising from grain refinement, a well known phenomenon in metal polycrystals. Indeed, this effect has been considered to be the essential factor for the M_s dependence on the grain size in steels.^{10,11}

As evident from the above summary, there are many factors which may influence the martensitic transformation. However, relative importance of these factors, which may be different from one system to another, is not known. The objective of the present study is to measure the dependence of the martensitic transformation on the grain size in Ce-TZP and to search for the most likely factor controlling the martensitic transformation of this particular system. The system was chosen because of its easiness in controlling the grain size by heat treatment and the martensitic transformation by cooling or stressing. In addition, the structure is most simple among the three types of transformation toughened ceramics.

2. Experimental Procedure

The starting material was ZrO₂-12mol%CeO₂ powders produced by a coprecipitation method (Daiichi Kigenso Kagakugogyo Co., Ltd., Osaka); the chemical compositions and powder characteristics are summarized in Table 1. The powders were mixed with an appropriate amount of acrylic binder followed by spray drying, CIPping, and dewaxing of the binder. Sintering was carried at three different temperatures (1400, 1450, and 1500°C) for 2h in air. The final size of the sintered plate was approximately 6 × 45 × 140mm. In order to obtain larger grain sized specimens, some of the 1400°C-sintered plates were annealed at various temperatures between 1550 and 1750°C for 2h in air.

Table 1. Composition(in wt %) and characteristics of the powders

ZrO ₂	CeO ₂	CaO	Na ₂ O	H ₂ O	Al ₂ O ₃	ig. loss	S.A* ¹	A.P.S* ²
82.44	15.98	0.004	0.003	0.52	0.19	0.46	33.7m ² /g	0.51 μm

*1 Specific surface area

*2 Average particle size

It was noted that plates heated at higher temperatures exhibit greenish color. The coloring indicates a partial reduction of the oxides, but a complete oxidation can be easily attained by annealing at a temperature near 1200°C for a short period.

From these plates specimens of various sizes were prepared for experiments. The cut surfaces were machine ground and followed by polishing on a metal disk with diamond emulsion of 9, 3, and 1μm powders, successively, and finally on a buff cloth with 1μm diamond powders. These ground/polished specimens were customarily annealed at 1400°C to remove the work-affected surface layer and also to oxidize to the stoichiometry.

Density was measured with Archimedean method. Grain sizes were obtained by measuring 100 grain intercepts with straight lines on scanning electron micrographs and multiplying the average by a geometric conversion factor 1.74.¹² Microvickers hardness was measured using a 1.96N load: average was taken over 20 measurements. Dynamic hardness tests were also made for some specimens. Lattice parameters and monoclinic/tetragonal phase content were measured by X-ray diffractometer with a Co K_{α} radiation and a graphite monochromator. When accurate lattice parameters were desired, peaks were step-scanned and

analysed using a peak fitting program.¹³ A correction for the sample displacement using the extrapolation function, $\cos \theta \cot \theta$, resulted in the reproducibility of a lattice parameter within 5×10^{-5} nm. An m-phase content was obtained using the following equations¹⁴

$$v_m = \frac{1.311X_m}{1 + 0.311X_m} \quad (1a)$$

and

$$X_m = \frac{I_m(\bar{1}11) + I_m(111)}{I_m(\bar{1}11) + I_m(111) + I_t(111)} \quad (1b)$$

where I_m and I_t are the integrated intensities of the respective peaks. Forward and backward transformation behavior was also measured by X-ray diffractometer attached with a cooling and heating stage, and also by a more convenient dilatometric method.

Three point bending tests were made at room temperature and at some selected temperatures below room temperature. The tests were carried out to meet JIS specification (JIS R1601, span length = 30mm and specimen cross section = 3×4 mm). Electron microscopic observation was made to see if there is any structural differences in the specimens heated at different temperatures.

3. Results

Before investigating into the effect of grain size on the martensitic transformation, the initial state of specimens with various grain sizes was characterized. The grain sizes and bulk densities are plotted *vs* the firing (sintering or annealing) temperatures in Fig. 2. Grain morphology is presented in Fig. 3 for selected specimens. When sintered at relatively low temperatures, specimens exhibited fine and regular equiaxial grains with little voids. With an increase of firing temperature, the grains markedly coarsened and large voids became outstanding, resulting in significant de-densification. The latter phenomenon was not expected at the beginning, since in most ceramics densification proceeds with an increase of firing temperature. Although detailed mechanism was not clear, it was suspected that the oxygen gas evolution during a partial reduction at high temperatures resulted in the voids. Unfortunately, once these large voids were formed, they could not be removed by annealing at a lower temperature where absorption of oxygen occurred until the stoichiometry was attained.

An X-ray phase analysis revealed that all specimens were essentially tetragonal except for those fired at 1750°C. Although a small amount of the m-phase was observed on the surfaces of the specimens sintered at 1450 and 1500°C, this could be readily removed by grinding and polishing or by annealing at 1400°C.

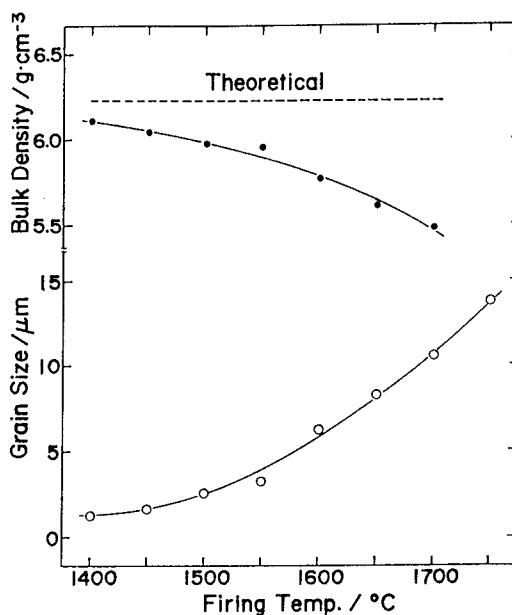


Fig. 2 Variation of the grain size and bulk density with firing temperature.

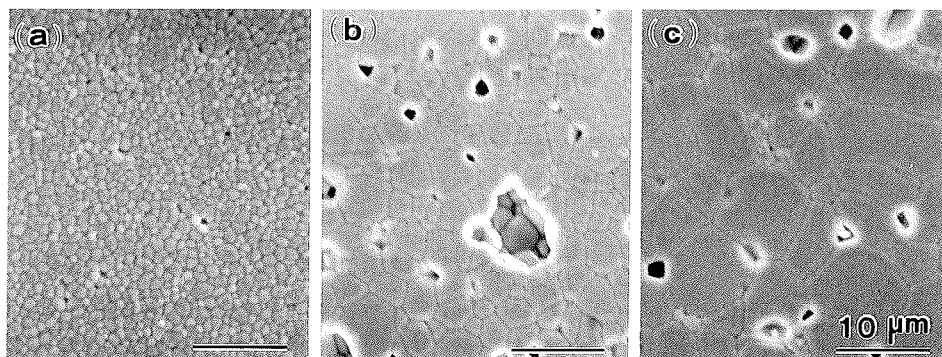


Fig. 3 Scanning electron micrographs showing the grain growth and voids formation for specimens fired at 1450°C (a), 1600°C (b), and 1700°C (c).

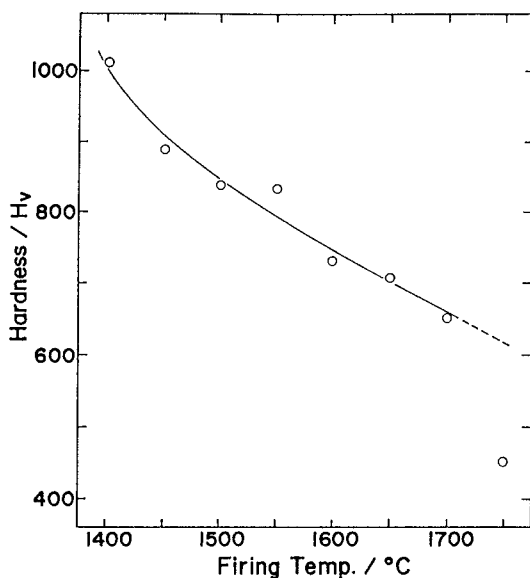


Fig. 4 Variation of the hardness with firing temperature. All specimens except for that fired at 1750°C were fully tetragonal.

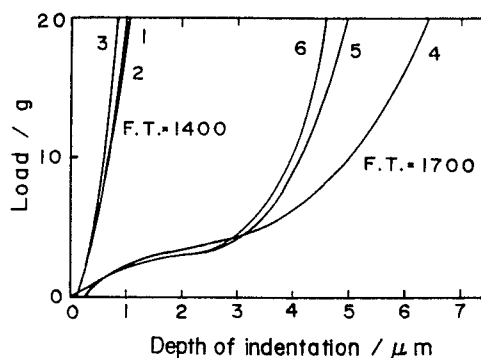


Fig. 5 Dynamical hardness measured for the specimens fired at 1400 and 1700°C. Three measurements were made for each specimen.

On the other hand, the specimens heated at 1750°C contained 83% and 51% of the m-phase on the surface and inside of the body, respectively. The plates heated at 1750°C were frequently accompanied with the cracks which were considered to be generated by the t→m transformation during cooling.

Microhardness is plotted in Fig. 4 against the grain size. The hardness decreased significantly with grain growth. The much lower hardness for the largest grain size (specimen heated at 1750°C) than the value expected from an extrapolation is due to the high m-phase content. Apart from the specimen heated at 1750°C, the indentations were not associated with microcracks at the indentation corners, nor

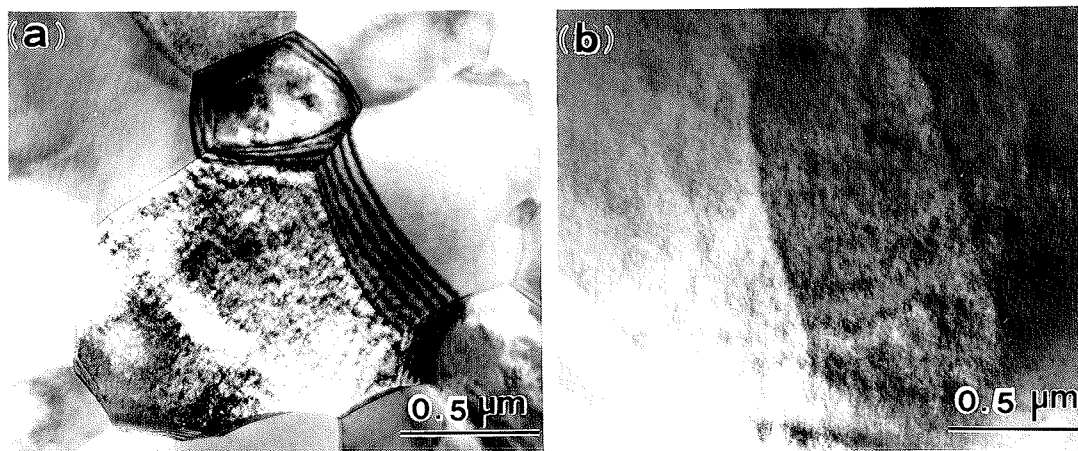


Fig. 6 Transmission electron micrographs showing fuzzy mottled structure in the specimens fired at 1450°C(a) and 1750°C(b). No significant difference was noted with different firing temperatures.

with any sign of extensive transformation such as a rosette pattern reported by Hannink *et al.*¹⁵ In these measurements, the size of indentation varied from 19 μm for the hardest specimen ($d \sim 1.3\mu\text{m}$) to 24 μm for the softest ($d \sim 10\mu\text{m}$). Since the size of indentation is significantly larger than the grain size, the measured hardness may well be considered to be representing the average hardness of the polycrystals rather than the matrix free from the effect of grain boundaries. The results of dynamic hardness tests are shown in Fig. 5. It is seen that the hardening behavior is considerably different between the specimens fired at 1400 and 1700°C. In the former the hardness rises quite steeply from the beginning, while in the latter the hardness goes through a plateau before rising steeply.

In order to examine other factors which may cause the hardness difference, microstructure was examined by electron microscopy. Typical structures are shown in Figs. 6(a) and (b) for the specimens fired at 1400 and 1700°C, respectively. In consistent with X-ray results, only t-phase grains were observed in both specimens as revealed by (odd, odd, even) extra spots characteristic to the phase.¹⁶ Despite the fully tetragonal phase, the matrices were not exactly featureless, instead fuzzy mottled contrast was noted in both specimens. Similar fine structures were often observed in zirconia alloys including specimens rapidly quenched from the melt.¹⁷ Even though the nature of these fine structure is not known, the appearance was the same for the two specimens. Precise lattice parameter measurements resulted in a slight difference between these two specimens, i.e., a and c are 0.51289 and 0.52228nm, respectively for the specimen fired

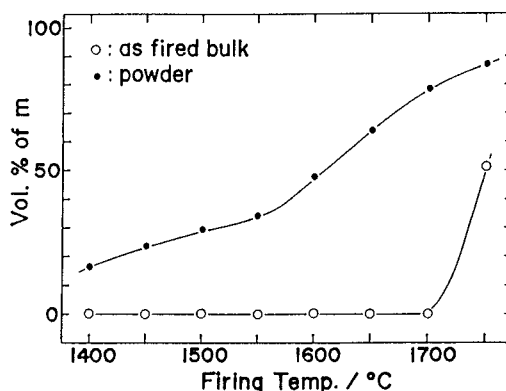


Fig. 7 The m-phase content in as-fired specimens and the the ground powders vs firing temperature.

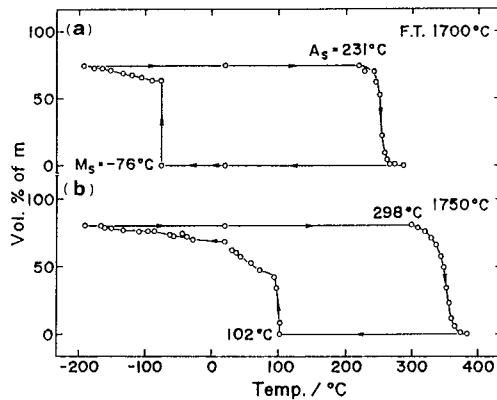


Fig. 8 Transformation cycles measured by X-ray diffraction for specimens fired at 1700°C (a) and 1750°C (b).

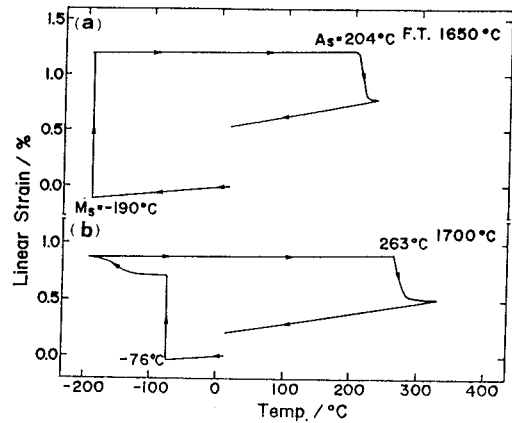


Fig. 9 Transformation cycles measured by a dilatometer for specimens fired at 1650°C (a) and 1700°C (b).

at 1400°C and the corresponding values for the 1700°C-specimen are 0.51230 and 0.52149nm, respectively.

Now we describe the effects of grain size on the martensitic transformation. A preliminary cooling experiment showed that only specimens fired at and above 1650°C underwent the $t \rightarrow m$ martensitic transformation when dipped into liquid nitrogen. In order to see the grain size effect in a wider range, a portion of each group of the specimens was ground into powders. The amount of mechanically induced m-phase was measured on the powders sieved through 44 μm meshes. As illustrated in Fig. 7, transformation was induced in all specimens but the amount of the m-phase monotonically increased with grain size.

For those specimens with M_s above liquid nitrogen temperature, transformation behavior was measured through forward and reverse transformations by using X-ray diffraction and dilatometric methods. Figures 8(a) and (b) show the result of X-ray measurements for the specimens fired at 1700 and 1750°C, respectively. The specimen fired at 1650°C failed to transform on the cryostat used, which enabled a specimen to cool to -192°C , even though transformation did occur when the specimen was directly immersed in liquid nitrogen.

The specimen fired at 1700°C was first cooled from room temperature (see Fig. 8(a)). The transformation took place at -76°C and 63% m-phase was formed with a burst. Further cooling increased the m-phase gradually and the amount reached 75% at -192°C . Heating to room temperature and further above caused no change below 231°C, then a rather rapid decrease of the m-phase occurred within a small temperature interval. At 286°C the reversion was completed.

In the case of the specimen fired at 1750°C, the cycle started with 69% m-phase at room temperature. Cooling to -192°C resulted in a gradual increase to 80%. By heating, the reverse transformation started at 298°C and completed at 384°C. When this was cooled to room temperature, a first burst occurred at 102°C followed by smaller bursts within a 10°C interval, then more gradual increase to 62% at room temperature.

Results of similar experiment but with a dilatometer are shown in Figs. 9(a) and (b). With this method, the specimen fired at 1650°C did transform, but for the specimen fired at 1750°C measurement

could not be made, because a standard procedure of annealing the machined specimen at 1400°C caused shattering during the cooling to room temperature. Quite a large burst was observed at -190°C for the specimen fired at 1650°C. No more transformation could be induced because the temperature could not be lowered below liquid nitrogen. By heating, the reversion started at 204°C and completed at 235°C. Cooling to room temperature failed to close the loop, which was due to the microcracks induced by the burst transformation. It was also noted that the slopes were different in the linear sections where no transformation was expected. The very small slope observed in the heating region after transformation was attributed to the small thermal expansion coefficient of the m-phase ($\sim 0.9 \times 10^{-6}/^{\circ}\text{C}$). But the difference between the initial slope before transformation and the final slope after reversion could not be explained. A comparison with the literature data⁸ ($\sim 7.5 \sim 13 \times 10^{-6}/^{\circ}\text{C}$) suggested that the slope of the latter was more agreeable. The smaller slope at the beginning may be an artifact caused by initial instability of the measuring system. If we assume that the presence of microcracks do not influence the thermal expansion, we can estimate the amount of transformation by taking the difference between the strains of the m-state and the final t-state both measured at room temperature. The unit cell expansion by the $t \rightarrow m$ transformation was calculated to be 4.7% from the lattice parameters. Since the observed linear strain was 0.67% or volume expansion of 2%, 43% of the m-phase was estimated to have been formed.

The data for the specimen fired at 1700°C (Fig. 9(b)) is similarly interpreted. The M_s and A_s agree with the X-ray result in Fig. 8(b). The amount of transformation estimated in the similar method as above was 39%, which is smaller than the X-ray result (63%). The difference suggests preferential transformation on the surface over the inside. The variation of M_s and A_s with grain size will be discussed later along with transformation temperatures under applied stress.

In the bending tests, two types of stress-deflection curves were observed, as illustrated in Fig. 10(a) and (b). Most of the specimens were fractured without any sign of yielding (a); whereas only the specimens fired at 1700°C and tested at -40°C showed a clear yielding followed by work hardening with serrations. The latter specimens exhibited marked transformation bands on the surface of tensile stress and also on the side surfaces, as shown in Fig. 11(a) and (b).

Results of fracture strength are plotted in Fig. 12. The data at room temperature, -83, and -196°C were the average of 3 or 4 tests, whereas the remaining data at intermediate temperatures were obtained from a single test. It is noted that strength is generally higher for fine grained specimen and for a fixed grain size the strength goes through a maximum with temperature variation, although for large grain sizes the maximum shifted above room temperature.

A similar variation of yield stress with temperature has been observed in metals which undergoes a stress-induced martensitic transformation.¹⁸ In metals, the region with a negative slope with temperature

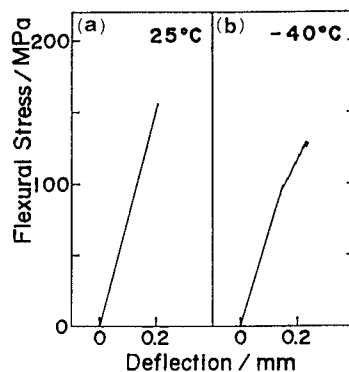


Fig. 10 Two types of stress-deflection curve obtained at 25°C (a) and -40°C for specimens fired at 1700°C (b). Specimens fired at different temperatures fractured without yielding at all test temperatures.

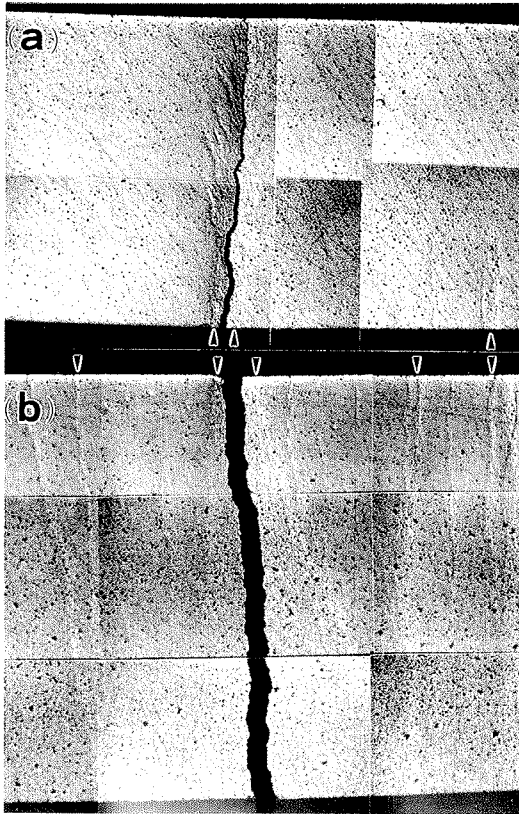


Fig. 11 Optical micrographs showing transformation bands near fracture surface (indicated by arrows) for a specimen fired at 1700°C and fractured at -40°C. (a) and (b) show a side surface (compression side up) and the bottom surface (tension surface), respectively.

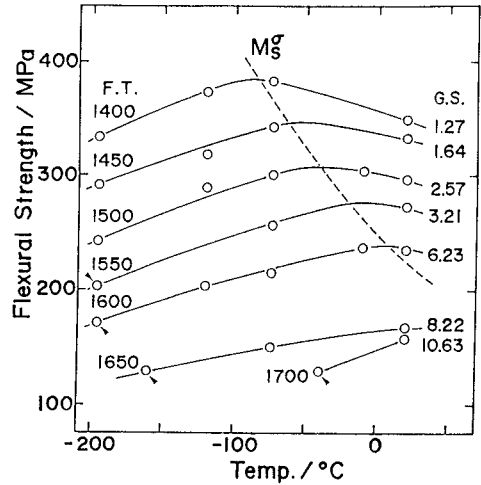


Fig. 12 Variation of the flexural strength with test temperature and firing temperature. F.T. demotes the firing temperatures in °C and G.S. the grain size in μm. M_s^σ is defined by the peak strength. Arrowheads indicate the specimens on which transformation bands were formed.

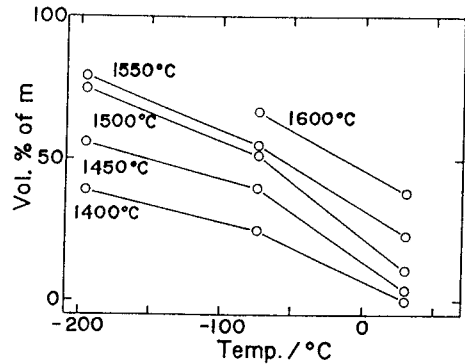


Fig. 13 Volume % of the m-phase on the fractured surface measured by X-ray diffraction method.

represents the usual temperature dependence of plastic flow stress, while that of a positive slope arises from stress-induced transformation yielding. The temperature corresponding to the peak strength, which is denoted by M_s^σ , lies in between M_s and M_d , the transformation temperatures by deformation. When an applied stress is increased a specimen at a temperature between M_s and M_s^σ yields by transformation (stress-induced transformation), while at a temperature between M_s^σ and M_d the specimen first yields by plastic deformation and a further increase in the strain induces martensitic transformation (strain-induced transformation).

Despite the apparent similarity to the shape of the stress-temperature curve of metallic system, the absence of yielding before fracture in the present case requires some consideration in the process involved in the regions of different sign of slope. The positive slope with temperature below a peak strength must be due to the stress induced transformation as in a metallic system. Since evidence for the transformation yielding was not obtained on the stress-strain curves except for one case, we looked for transformation bands on the specimen surface as alternative evidence, but we could find it only in a part of the specimens fractured in the temperature range of a positive slope, as indicated by arrows in Fig. 12. Even though we failed to provide direct evidence, we believe the positive slope itself is a piece of evidence for the stress-induced transformation.

On the other hand, the region of a negative slope must be representing the usual temperature dependence of fracture strength. As illustrated in Fig. 13, even on the specimens fractured in this region exhibited the m-phase on the fracture surface. But this m-phase was likely to be formed by the high stress field around the tip of a propagating crack. Thus the m-phase should be referred to as *crack-induced* martensite rather than strain-induced martensite.

Since we could not distinguish between stress-induced and crack-induced transformation by direct observation, it is not clear whether the transition occurs abruptly at the peak strength or more gradually over some temperature range. Nevertheless, the temperature giving the peak strength would be representing some measure of the stability of the parent against the martensitic transformation. Thus following the convention of a metal case, we tentatively define M_s^σ by the temperature giving the peak strength and M_d by the temperature where the m-phase was first detected on the fracture surface. As seen in Fig. 12, M_s^σ so defined exhibits a marked dependence on the grain size.

4. Discussion

The variations of M_s and A_s obtained from Figs. 8 and 9 and M_s^σ estimated from Fig. 13 are plotted in Fig. 14 vs grain size. Despite the scarcity of the data, marked grain size dependences are noted for all three characteristic temperatures. The broken line indicates an expected variation of M_d . The line was drawn through the known M_d point for the smallest grain size and parallel to M_s^σ assuming that it varies similarly with grain size.

The present specimens were intended that they differ only in the grain size. Examinations were made to see if this requirement was satisfied. One obvious variation, besides the grain size, was the amount and size of the voids. We also noted that specimens fired at higher temperatures tended to lose some oxygen as evident from the coloring. Even though quantitative measurement of the oxygen deficiency was not made, annealing of the specimens before tests must have brought the specimens back to the stoichiometric composition. The appearance of the fuzzy mottled structure was intriguing, since

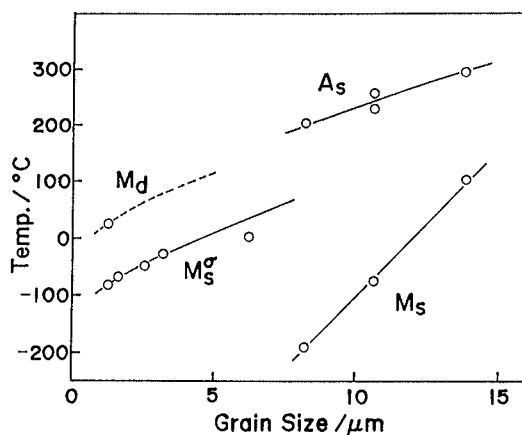


Fig. 14 Variation of the characteristic temperatures of the transformation with grain size.

no phase decomposition was expected with the presently employed heat treatments according to the phase diagrams in the literature.¹⁹ In zirconia systems, fine structures of the similar kind have been often observed,¹⁷ but their origins are not fully understood. Fortunately no significant differences were noted in the microstructure of the specimens fired at different temperatures. We also observed that the tetragonal lattice parameters of the specimens fired at 1700°C was 0.1 % smaller than that fired at 1400°C. Even though the difference is small, it may indicate a small difference in the composition. Only possible reason for the composition change is the evaporation of cerium during firing at a high temperature. However, even in the specimens fired at the lower temperatures where no evaporation was expected, we still observed a change in M_s^σ with the firing temperature (or grain size). Thus, the effect of the composition change should be small if there was any. The size of voids is known to lower the fracture strength of brittle materials. Thus the present results of the bending tests were likely to have been influenced by the voids. However, it should be noted that the present M_s^σ were determined from the temperature giving a peak strength and they should not be influenced by the absolute strengths. For the hardness measurements, the void were not expected to influence the measurements as we could avoid large voids for indentation.

So long as the the microstructure remained essentially the same apart from the grain size, the significant hardness variation is attributed to the difference in the grain size. The difference in the initial hardening rate with different grain size observed in the dynamical hardness tests appears to support this. A hardening effect by grain refinement is well known in metals and the phenomenon is usually accounted for by the dislocation mechanism put forward by Hall²⁰ and Petch.²¹ Although the mechanism may not be the same in ceramics, analogous strengthening effects by grain refinement are commonly observed.²²

Although there remains some ambiguities concerning the presence and the role of incidental differences which may have been brought into the specimens by the different firing temperatures, we assume that they do not play a predominant role. Then the present variation of the transformation temperatures with grain size is most naturally interpreted by the strengthening effect caused by the grain refinement. This concept has been originally put forward by Ansell and his coworkers¹⁰ to account for the grain size dependence of the M_s in steels and later supported by Kajiwara.¹¹ According to these authors, a martensitic nucleation requires plastic accommodation of the surrounding matrix, and the work necessary for the process is thus dependent on the average strength of the material. Thus when the matrix is strengthened a larger driving force must be exerted by further cooling the specimen.

Other possibilities reviewed in Sec. 1 can be mostly ruled out for this particular system. An exception is the possibility of stress concentration arising from thermal expansion anisotropy,⁸ which is expected from the tetragonal symmetry of the present specimens. Still further, a small composition variation owing to the exposition to a high temperature cannot be completely ruled out.

Finally the relative magnitude of the characteristic temperatures in Fig. 14 is discussed. The following inequality relations are customary assumed:

$$M_s < M_s^\sigma < M_d < T_0 < A_d < A_s \quad (2)$$

where A_d (not measured) denotes the temperature where reverse transformation starts under deformation, others have been defined previously. Furthermore the following relations are assumed to approximately hold:

$$\frac{M_s + A_s}{2} = \frac{M_d + A_d}{2} = T_0 \quad (3)$$

The latter relation is frequently used to estimate T_0 . By definition, T_0 should not vary with grain size. Then we immediately see that no horizontal line for T_0 can be drawn in Fig. 14 satisfying the relations

(2) and (3). The apparent inconsistency of the data with the relations (2) and (3) indicate that these relations are not physically sound, though often satisfied. In particular there seem to be no physical basis for the inequality:

$$T_0 < A_s$$

This may be explained as follow: A transformed region and its surrounding are in a state of residual stress, which has the sense that helps the reverse transformation. When the back stress becomes very high, A_s can be lowered, even below T_0 . The magnitude of the residual stress may well depend on the strength of the material. Thus, the present martensite formed at low temperatures, where the matrix is strengthened by both grain refinement and the low temperature, should result in quite high residual stress. For these reasons, the current data are indeed consistent with physical requirements.

5. Summary and Conclusions

Specimens of various grain sizes were prepared from 12mo%CeO₂-TZP. On these specimens, characteristic temperatures for the t↔m transformation, such as M_s , A_s , and M_s^σ , were measured by cooling/heating cycles or bending tests at low temperatures. Hardness and microstructure were also examined. Both M_s and M_s^σ , as well as A_s , decreased but the hardness increased with grain refinement, while the microstructure remained essentially the same. The data allowed the following conclusions to be made.

1. The primary origin of the stabilization effect by grain refinement in Ce-TZP is the strengthening effect caused by the grain refinement.
2. The reduction of A_s with grain refinement can be accounted for by the larger back stress associated by the plastic deformation of the matrix of a higher strength.
3. The residual stress at facet corners arising from the thermal expansion anisotropy and a slight change in the composition may also have some influence on the variation of the transformation temperatures of the present system.

Acknowledgement

We wish to thank Mr. S. Mishima at Industrial Research Laboratory, Tottori Prefecture, for making dynami micro-hardness tests.

References

1. R. C. Garvie, R. H. Hannink, and R. T. Pascoe, "Ceramic steel?", *Nature*, **258**, 703-4 (1975)
2. T. K. Gupta, J. H. Bechtold, R. C. Kuznicki, and L. H. Cadoff, "Stabilization of Tetragonal Phase in Polycrystalline Zirconia", *J. Mater. Sci.*, **12**, 2421-6 (1977)
3. N. Claussen, "Fracture Toughness of Al₂O₃ with an Unstabilized ZrO₂ Dispersed Phase", *J. Amer. Ceram. Soc.*, **59**, 49 (1976)
4. A. G. Evans, N. Burlingame, M. Drory, and W. M. Kriven, "Martensitic Transformations in Zirconia-Particle Size Effects and Toughening", *Acta metall.*, **29**, 447-56 (1981)
5. F. F. Lange, "Transformation Toughening Part 1 Size Effects Associated with the Thermodynamics of Constrained Transformations", *J. Mater. Sci.*, **17**, 225-34 (1982)
6. R. C. Garvie and M. V. Swain, "Thermodynamics of the Tetragonal to Monoclinic Phase Transformation in Constrained Zirconia Microcrystals Part 1 In the Absence of an Applied Stress Field", *J. Mater. Sci.*, **20**, 1193-200 (1985)

7. C. A. Anderson and T. K. Gupta, "Phase Stability and Transformation Toughening in Zirconia", pp. 184-201 in *Advances in Ceramics 3, Science and Technology of Zirconia*. Edited by A. H. Heuer and L. W. Hobbs. American Ceramic Society, Columbus, Ohio, 1981
8. A. H. Heuer, N. Claussen, W. M. Kriven, and M. Rühle, "Stability of Tetragonal ZrO₂ Particles in Ceramic Matrices", *J. Amer. Ceram. Soc.*, **65**, 642-50 (1982)
9. R. H. J. Hannink, "Growth Morphology of the Tetragonal Phase in Partially Stabilized Zirconia", *J. Mater. Sci.*, **13**, 2487-96 (1978)
10. T. J. Nichol, G. Judd, and G. S. Ansell, "The Relationship between Austenite Strength and the Transformation to Martensite in Fe-10pct Ni-0.6 pct C Alloy", *Metall. Trans. A*, **8A**, 1877-83 (1977)
11. S. Kajiwara, "Roles of Dislocations and Grain Boundaries in Martensite Nucleation", *Metall. Trans. A*, **17A**, 1693-702 (1986)
12. A. W. Thompson, "Calculation of True Volume Grain Diameter", *Metallogr.*, **5**, 366-9 (1972)
13. M. Hayakawa and M. Oka, "XPKFIT: Peak Separation with Arbitrary Relations Among the Component Peaks", *J. Appl. Cryst.*, **14**, 145-48 (1981)
14. H. Toraya, M. Yoshimura, and S. Sōmiya, "Calibration Curve for Quantitative Analysis of the Monoclinic-Tetragonal ZrO₂ System by X-Ray Diffraction", *J. Amer. Ceram. Soc.*, **67**, C119-21 (1984)
15. R. H. J. Hannink and M. Swain, "Metastability of the Martensitic Transformation in a 12 mol% Ceria-Zirconia Alloy: I, Deformation and Fracture Observations", *J. Amer. Ceram. Soc.*, **72**, 90-98 (1989)
16. G. Teufer, "The Crystal Structure of Tetragonal ZrO₂", *Acta Cryst.*, **15**, 1187 (1962)
17. M. Hayakawa, K. Adachi, and M. Oka, "Tweed Contrast with (223) Habit in Arc-melted Zirconia-Yttria Alloys", *Acta metall. mater.*, **38**, 1761-67 (1990)
18. I. Tamura, "Deformation-induced Martensitic Transformation and Transformation-induced Plasticity in Steels", *Metal Science*, **16**, 245-53 (1982)
19. E. Tani, M. Yoshimura, and S. Sōmiya, "Revised Phase Diagram of the System ZrO₂ - CeO₂ below 1400 deg C", *J. Amer. Ceram. Soc.*, **66**, 506-10 (1983)
20. E. O. Hall, "The Deformation and Ageing of Mild Steel: III Discussion of Results", *Proc. Phys. Soc. B*, **64**, 747-53 (1951)
21. N. J. Petch, "The Cleavage Strength of Polycrystals", *J. Iron and Steel Inst.*, **174**, 25-28 (1953)
22. W. D. Kingery, H. K. Bowen, and D. R. Uhlman, "Introduction to Ceramics", Chapt. 10, John Wiley & Sons, New York (1976)